Medical Image Analysis (1999) volume 3, number 3, pp 265–274

Evaluation of robot-based registration for subtraction radiography

Grigore C. Burdea[1,2]*, Stanley M. Dunn[2] and Guy Levy[3]

[1]Rutgers University, Electrical and Computer Engineering Department, 94 Brett Road, Piscataway, NJ 08854-8058, USA
[2]Rutgers University, Biomedical Engineering Department, 617 Browser Road, Piscataway, NJ 08854-8014, USA
[3]AT&T Laboratories, 307 Middletown, Rm 3D-344, Lincroft Rd, Lincroft, NJ 07738, USA

Abstract
Digital subtraction of (plane film) radiographs of an area of interest taken over time is a powerful diagnostic tool. In dentistry for example, this is used to detect and treat periodontal disease (i.e. the sequence of diseases that leads to the loss of bone supporting the teeth). A precondition of subtraction radiography is correct three-dimensional registration of the film and X-ray source, without which the subtraction images are meaningless. A small misalignment can be compensated for by post-processing of the digitized films (by correspondence and rectification) to remove artifacts due to positioning errors. This paper presents a novel approach to subtraction radiography which replaces customary mechanical alignment methods (such as a stent or cephalostat) with a robot. A mechanical stent is a short rod attached at one end to the X-ray source and at the other to a mechanical appliance protruding from the patient's mouth. An experimental system was constructed which creates a 'sensorized stent' by integrating a plastic mouth appliance (with the impression of the patient's teeth), a robot carrying an X-ray source and a host computer. Results showed that the robotic system was superior to the mechanical alignment approach, due to its excellent accuracy and repeatability. This resulted in much less variation in the non-registered X-ray images, and in a smaller standard deviation in the intensities of subtracted images overall. The results suggest that in the future, diagnostic studies including subtraction radiography will not need either mechanical alignment (which is imprecise) or post-processing registration (which is time consuming).

Keywords: dental radiograph, image registration, robot, subtraction radiography, tracking

Received May 15, 1998; revised November 4, 1998; accepted January 18, 1999

1. INTRODUCTION

Subtraction radiology, first described by Zierdes des Plantes in 1935, uses optical subtraction of different radiographs in order to remove anatomical areas which are not of interest (Curry, 1984). The removal of this so-called structured noise makes changes in the area of interest easier to see.

In dentistry minute changes in the mandibular bone structure occurring over time may mean the onset of periodontal disease; for more details on periodontal disease see Brown and Loe (1993) and Genco and Loe (1993). Its early detection relies on dental radiographs (analog or digital) which have the inherent limitation that they provide only a two-dimensional (2-D) projection (i.e. view) of the area of interest. If the bone loss is not caught in time, the result can be tooth loss and continued oral health problems (Dunn *et al.*, 1999).

The presence of changes in the bone structure supporting the teeth triggers changes in the X-ray film (or image) intensity. Studies have shown that the subtraction of X-rays of the dental area of interest taken over time under ideal conditions helps in the diagnosis of periodontal disease

*Corresponding author
(e-mail: burdea@vr.rutgers.edu)

(Braegger, 1988, Braegger *et al.*, 1989). Ideal conditions refer to those conditions under which the three-dimensional (3-D) alignment of the X-ray source, area of interest and film (or X-ray sensor) is exactly the same in both radiographs that are being subtracted to highlight change. If the alignment condition is not met, then the images of an unchanged bony area will be confounded by differences due to image registration error, and subtraction radiography is meaningless.

It is thus necessary to standardize the views of the area of interest in repeated radiographs taken over time. This is not an easy task and several approaches have been used to solve the alignment problem. Earlier work used mechanical devices such as stents and cephalostats to fix the patient and X-ray source relative position (Ortman *et al.*, 1985; Rethman *et al.*, 1985). A mechanical stent is a short rod attached at one end to the X-ray source and at the other to a mechanical appliance protruding from the patient's mouth. Unfortunately, such mechanical alignment is uncomfortable for the patient and impractical for certain tooth positions.

A more recent approach to imaging standardization needed in subtraction radiography is the use of image registration software in the post-processing of digitized X-ray film (Dunn, 1993; Fisher *et al.*, 1995; Ostuni *et al.*, 1995; Versteeg *et al.*, 1995). The approach uses projective invariants in the two images, which are characterizations of stable anatomical features not affected by normal or pathological changes that may have occurred between exposure of the two subsequent images. By manually selecting feature points in the digitized image it is possible to force geometric correspondence, as long as the relative 3-D translation and/or rotation of the two images is within bounds. Misalignment of the non-registered images is thus limited to <16 mm translation and 16° rotation. Even within these constraints it is intuitive that the image registration prior to subtraction will work better if the two X-rays are well aligned to begin with. For details of the mathematical model and the rectification procedure based on projective invariants, please see Dunn (1993).

A novel approach to dental image alignment proposed by Burdea and colleagues (Burdea *et al.*, 1991, 1992) was the use of a sensorized mouth appliance tracked by a robot carrying the X-ray source. By coupling an accurate 3-D tracker and a repeatable robot the researchers predict that image standardization is possible without any mechanical devices. The present article is a continuation of the earlier concept paper through actual implementation of the system utilizing an industrial robot and a standard X-ray source. The objective was to improve image standardization such that subsequent image registration (the step precursor to subtraction) is always feasible. Experimental data was obtained on registration image quality by comparing the traditional mechanical stent approach to the robotic system. Test results showed the robotic system to be superior to the stent approach in image standardization which led to better image registration. Section 2 presents the hardware and system software used in the present study. Section 3 describes the dental subtraction radiography software interface used. Section 4 presents the experimental results. Concluding remarks and future work directions are given in Section 5.

2. EXPERIMENTAL SYSTEM

The robot-based dental subtraction radiography system consists of a robot manipulator, its dedicated controller, a host computer, an X-ray system and a sensorized mouth appliance, as illustrated in Figure 1 (Levy *et al.*, 1994).

The robot used in the present experiment is a 270 kg Merlin Intelligent Robot System with six degrees of freedom for waist, shoulder, elbow, wrist rotation, wrist flexion and hand rotation (American Robot Co., 1985a). The use of such a massive manipulator was required to carry the large payload of the X-ray source which was retrofitted on its wrist. The robot controller has a distributed system of eight 6809 microprocessors and a central 8 MHz 68 000 microprocessor. It is responsible for robot kinematic computations (trajectory control), communication with the operator's console (VT 100 terminal) and with the host computer over an RS232 line.

The host computer is a Sun SparcStation 1 with grayscale monitor which is required to display digitized X-ray images. The host computer is in charge of the overall process management and user input/output. It communicates with the robot controller to receive status information and to issue motion commands, based on the 3-D position of the mouth appliance.

The sensorized mouth appliance is molded onto the lower jaw of a cadaver; it holds the X-ray film as well as the receiver of a 3-D tracker. These appliances are removable and put in place only when films are exposed. Repositioning the appliance introduces small errors in film placement with respect to the site of interest and these errors are correctable by the image standardization procedure.

The tracker used here is a Polhemus Fastrack magnetic tracker which has a control unit, a transmitter and a receiver. The relative position of the receiver (and thus of the mouth appliance) versus the transmitter is measured 120 times s^{-1}, and is sent by the sensor control unit to the host computer over a second RS232 line.

The mouth appliance is placed on a simple 2-D motorized platform which simulates the patient's head tilting and rotation motions at up to 28 r.p.m. The robot carrying the X-ray source tracks this motion based on the Fastrack information and the off-line measurement of the fixed position of the tracker relative to the dental film. Thus the host can

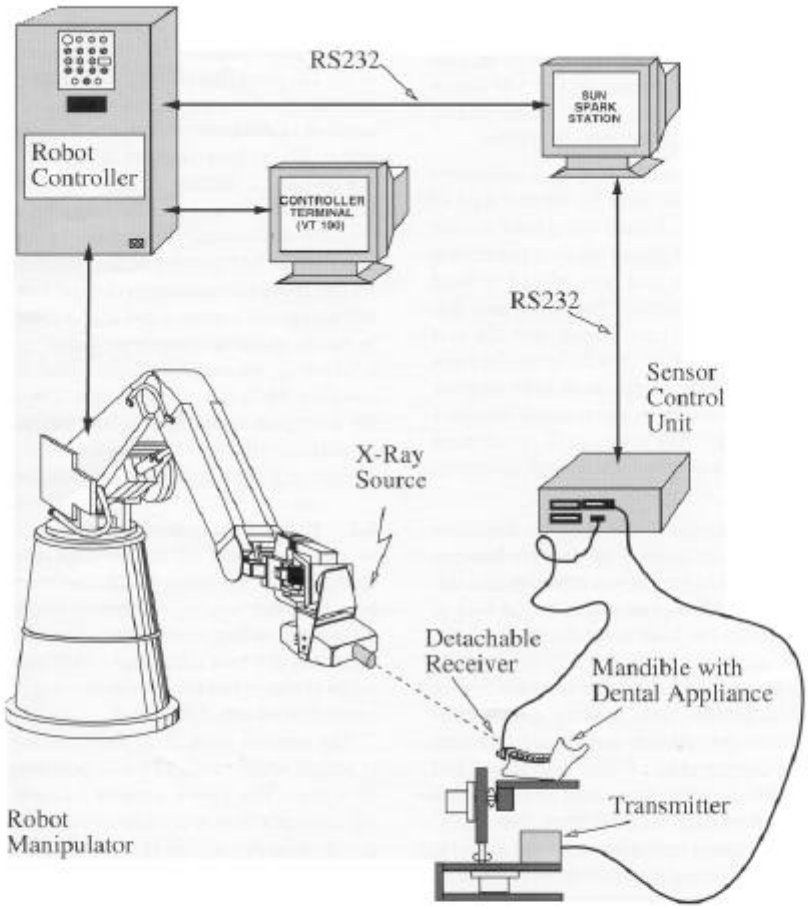

Figure 1. Robotic system for dental subtraction radiography (Levy *et al.*, 1994). (© Shadyside Hospital, reprinted by permission.

transmit film position information to the robot controller which maintains a fixed orientation between the X-ray source and film within a given work volume.

A General Electric GX-100 intra-oral X-ray source was attached to the robot wrist with a custom aluminum connector. The GX-100 master controller (not shown in Figure 1) allowed the manual setting of the duration and intensity of the X-ray emission once a hand switch was pressed. The X-ray system was modified from its standard configuration by wiring the hand switch to the robot controller's I/O ports. Thus the robot controller enabled the hand switch only when certain conditions were satisfied (as will be discussed later). The X-ray film used in our experiments was Kodak Ektaspeed dental film; it was developed with Kodak LX 24 developer and Kodak FX 4 filter.

Finally a safety switch was wired to the robot controller's I/O ports. This mechanical switch mimicked an external safety device, such as a mat, which would stop the system if a person was within the robot manipulator's reach. An alternative would be to install a light curtain to turn the robot manipulator off if the X-ray source head entered a restricted volume around the patient's position. Portable X-ray protection panels were installed around the perimeter to protect the researchers from accidental X-ray overexposure.

2.1. Tracking calibration

We consider tracking of the mandibular motion to be successful if the robot has accurate calibration, the 3-D sensor is sufficiently accurate and the motion data is transmitted by the host to the robot controller at sufficiently high rates.

Robot calibration was performed by placing a calibration fixture on the robot wrist coaxial with the central axis of the X-ray source. The calibration fixture was a laser pointer with eight adjustable attachments placed inside a transparent plastic cylinder. A calibration grid was placed a fixed distance away from the laser pointer. The robot arm was repeatedly moved to position the laser pointer over the grid intersections; thus it was possible to zero the errors in robot orientation and position, with the exception of wrist rotation, by comparing the known position to the position feedback from the Polhemus Fastrack. Any errors in X-ray rotation about the central ray will not affect the image geometry, which is invariant to these X-ray source rotations.

The second set of measurements was made to determine the 3-D tracker accuracy as a function of the distance between the magnetic source and the receiver. It was hypothesized that in a normal setting the source would be placed on the back of the patient's chair, opposite the head restraint. As such the distance to the mouth appliance holding the receiver would be ~20 cm or less. During the calibration tests the source was attached to a non-metallic table holding a millimeter grid on which the receiver was moved, and its measurements were compared to the correct ones. It was determined that the corresponding Euclidean (total) translation error was well under 1 mm, and the Euclidean rotation error was <0.5° (Dunn *et al.*, 1996). Subsequent measurements were aimed at quantifying the influence of dental restorations and orthodontic wire in the mandible on 3-D sensor measurements. This time the source–receiver distance was kept constant (20 cm), and measurements were made with and without the mandible being interposed between the source and the receiver. The difference between position measurements with and without the interposed mandible was then compared with the sensor electronic noise at that location. Subsequently the receiver was moved to another location on the 20 cm circle and the process repeated. The results showed that the maximum Euclidean translation difference of measurements with/without the mandible was only 0.12 mm, while the corresponding sensor noise was 0.1 mm. Similarly the maximum Euclidean rotation difference with/without the interposed mandible was 0.4° compared to a corresponding sensor noise of 0.31°. Thus the presence of dental restorations and orthodontic wire did not affect the 3-D tracker's accuracy, since the above differences were of the order of magnitude of the sensor noise.

Eventually the overall tracking error was determined by installing the magnetic receiver on a vertical calibration grid, at 20 cm from the source. The robot was commanded to track the motion (translation/rotation) of the sensor, while the position of the laser pointer was measured on the calibration grid. These tests showed an overall translation error of <1 mm and a rotation error of <1°. These errors are well below the limits of image registration software, thus it was possible theoretically to replace the mechanical stent with non-contact 3-D tracking of the mouth appliance.

The above measurements showed that the magnetic tracker had acceptable accuracy and repeatability for our application. In severe magnetic-interference environments an alternative is to use an ultrasonic tracker instead of a magnetic one. In this case the X-ray source output tube can be placed inside the triangular transmitter, while the receiver can be placed directly onto the mouth appliance. In this way the direct line of sight requirement of ultrasonic trackers is met.

2.2. Robot–host communication

A key component of the dynamic tracking of the mouth appliance by the robot is the communication between the host computer reading 3-D sensor positions and determining the corresponding robot target point, and the robot controller executing the host command. This communication process needs to assure fast robot response despite an RS232 effective bandwidth of only 2700 baud.

The process starts with the sampling of the Fastrack 3-D sensor which reads 120 new positions s^{-1} with a latency of 4 ms. The sensor current location is then mapped to the corresponding X-ray source location using homogeneous transformation matrices as in:

$$^{\text{base}}T_{\text{X-ray}} = {}^{\text{base}}T_{\text{frame}}\,{}^{\text{frame}}T_{\text{source}}\,{}^{\text{source}}T_{\text{sensor}}\,{}^{\text{sensor}}T_{\text{tooth}}\,{}^{\text{tooth}}T_{\text{X-ray}}.$$

Details of the above transformation matrices can be found in Burdea *et al.* (1991). A 'point server' process is in charge of reading the 3-D tracker information, converting it to a robot target position and placing it in a shared memory location. A second process in charge of communication with the robot controller reads a new point target after each robot move has been completed. Naturally, the two processes are asynchronous, with the point server process writing into shared memory much faster than the communication process can read. Thus inter-process communication is mediated by semaphores, which ensure that the shared memory data is not overwritten while being read for the robot controller.

The low baud rate of the RS232 line used to transmit data to the robot controller necessitates a data encoding scheme.

Table 1. Task communication protocol (Levy *et al.*, 1994). (© Shadyside Hospital. Reprinted by permission)

Control task	Packet type	Task	Label
N/A		Robot state query	S
N/A		Error state query	Q
N/A		Error state report	E
Motion		Enable robot	M
Motion		Disable robot	N
Motion		Calibrate robot	C
Motion		Home robot	H
Motion		Move robot to point	P
Motion		Reference frame definition	F
I/O		Enable I/O ports	I
I/O		Disable I/O ports	K
I/O		Enable sensor	S
I/O		Disable sensor	T
I/O		Enable X-ray	X
I/O		Disable X-ray	Y
I/O		Enable joystick	J
I/O		Disable joystick	L

By bringing the robot into the vicinity of the mouth piece prior to automatic control, it was possible to limit the size of the position/orientation data to only two bits each (encoded). Since the length of each data packet was fixed, it was possible to eliminate the wait bit, further improving communication speed. The point data encoding, together with shared memory management on the host computer, made possible a robot response time of only 0.64 s. This represents the average time it takes the robot to respond to a new position target, while moving at 1.52 m s^{-1}.

The tasks requested by the host computer refer to motion commands, but also to I/O operations, status checks or error reporting. Motion commands enable/disable the robot, 'home' the robot (move to a predefined position), calibrate the robot, move the robot to another point or define reference frames. I/O operations may enable/disable the X-ray manual switch, enable/disable the teach pendant for calibration or enable/disable the 3-D sensor which are all wired through the robot controller I/O ports. In order to speed up communications (and thus system response) the tasks are also encoded, forming a library of 19 single character symbols used by the host computer. The mapping of each of these characters to the corresponding robot task is shown in Table 1 (Levy, 1994).

On the robot side the flow control for new tasks is performed by a software dispatcher implemented as an infinite loop. Once a new task is received by the dispatcher, it is decoded and command is relinquished to the corresponding robot subroutine. These routines, written in AR-BASIC (American Robot Co., 1985b), return control to the dispatcher once execution is complete, and a new command is then read and decoded.

If errors occur during task execution the software dispatcher sends an error message to the host, for display on the user's graphical user interface (GUI). A similar message is also displayed on the controller terminal, for diagnostic purposes. All errors result in the disabling of the robot motion control.

2.3. Graphical user interface

A graphical user interface was created to allow operation of the robotic dental X-ray system by a non-technical person. The GUI integrates all software modules (AR-BASIC on the robot, RS232 communication, C on the 3-D tracker and host shared memory etc.) in a unified application. Additionally the GUI performs transparent error checking on user input, increasing overall system safety and reliability.

The SUN SparcStation 1 host computer had X Library widgets that were the basis of the GUI (Quercia and O'Reilly, 1993). The main application screen consisted of three pull-down menus and a status window as shown in Figure 2.

The first menu allowed the operator access to the patient database to load (*Open*) an existing patient's file. A patient's file contains the transformation matrix between the 3-D sensor and X-ray film for that particular patient. An opened patient file is a precondition for tracking to occur. The second menu allows the control of the robot holding the X-ray source.

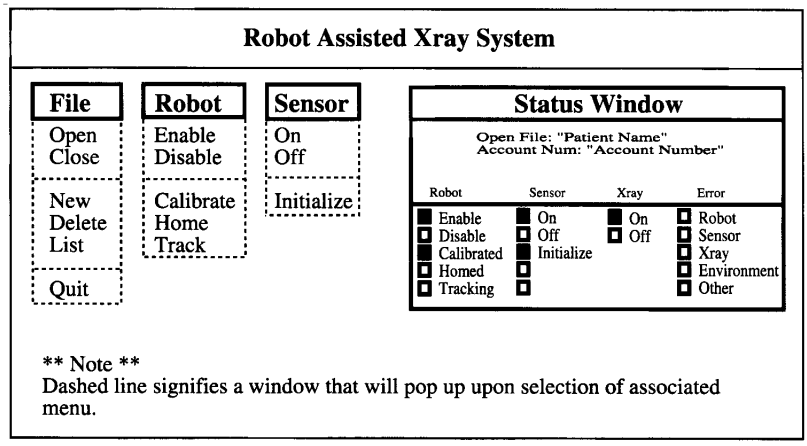

Figure 2. Robotic dental radiography GUI (Levy, 1994).

It allows the enabling or disabling of the manipulator motion control and starts the tracking process once the patient has been seated and the mouth appliance properly fitted. The third menu allows the operator to turn on the 3-D sensor remotely as a precondition of robot tracking.

The window displayed next to the pull-down menus informs the operator of the system status, namely the robot state, the 3-D sensor state and any error condition. Errors occur whenever the robot malfunctions, in case of a safety violation (a person on the safety mat or the emergency button pressed), or violation of task sequences. A special status window is displayed once the robot is in the 'tracking' mode, which then changes to 'locked' once the robot has placed the X-ray source in the correct geometric relationship to the X-ray film. In all other states the manual switch for taking X-rays is disabled.

3. SUBTRACTION RADIOGRAPHY USER INTERFACE

In this pilot study after the radiographs were exposed and processed, they were digitized to 240 × 256 pixels with 8 bits/pixel contrast resolution. Small variations in image contrast due to film processing were corrected using an algorithm described in Dunn *et al.* (1999). The digitization software was incorporated in the Motif-based subtraction radiography user interface (SRUI) illustrated in Figure 3 (Levy *et al.*, 1994).

The SRUI has five sub-windows, with the baseline radiograph being displayed in the upper left-hand corner of the screen. To the immediate right is the second (subsequent) radiograph of the same region of the mouth. The two images have small differences even if the area of the mouth they represent has not changed. These differences are due to small errors in alignment (due to calibration errors, or stent placement errors over time), and to digitization artifacts. The operator then manually selects anatomically stable features of interest in both images in order to rectify the second radiograph (i.e. to bring it into stereoscopic alignment) with the first. The registered image is then displayed in the lower left-hand sub-window. Subtraction of the rectified image from the baseline radiograph is then performed in order to highlight any bone loss or other anatomical changes that may have occurred in the time span between the two radiographs. The larger sub-window to the right allows the operator to double the size of any of the smaller sub-windows in order to better analyze the results.

The bottom of the SRUI is an information area used to display the coordinates of the corresponding feature points used in image registration. The same area displays the fundamental matrix (i.e. the 4 × 4 transformation matrix between the two images in homogeneous coordinates) used in image registration (Ostuni *et al.*, 1995) as well as the average and standard deviation in the subtracted image gray levels. An image control menu was created as part of the same SRUI in order to help the user in the selection of feature points. An 'image modification' window is displayed which allows

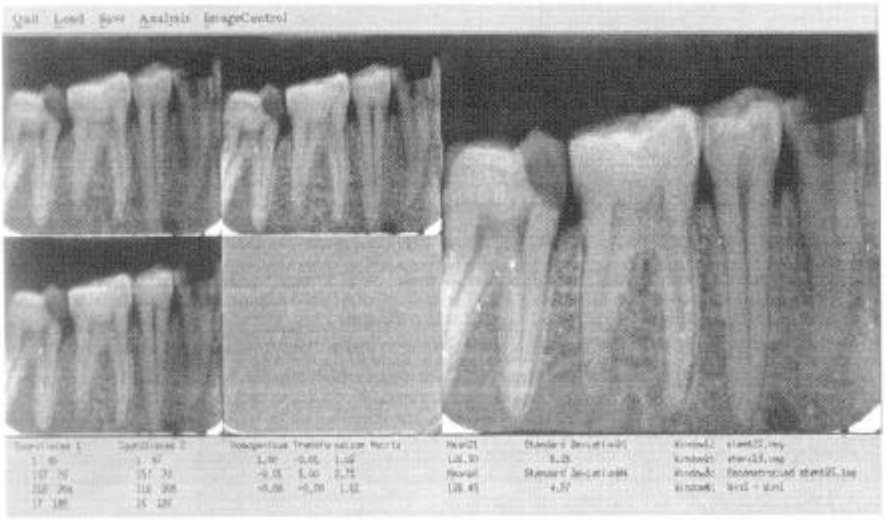

Figure 3. Subtraction radiography user interface (Levy *et al.*, 1994). (© Shadyside Hospital. Reprinted by permission.)

the user to change the brightness and contrast in the selected image. A histogram equalization routine can be used so that more values in the range 0–256 are used.

The subtraction window gives a very good indication of any change between the two images. If there is no change the subtraction result will be a uniformly gray sub-window, corresponding to a mean grayscale level of 127.5 and a standard deviation of zero. If changes exist, regions of bone growth will appear white, while areas of bone loss will appear dark.

With all the above advanced interface features the user should be able to correctly and accurately identify four feature points in the two images, which is a necessary precondition for the success of the registration algorithm. However, the more the two images differ in imaging geometry, the more difficult the user's task is to identify the corresponding features in the images. Even if the features are identified correctly, the registration software will fail if the two images are outside the convergence domain of the algorithm. This domain restricts relative translation between the two images to <16 mm, and relative rotation to be $<16°$. It is thus most important to start with two images that are quite similar in imaging geometry, so that registration is successful. The following section will show how the robotic system described above is able to satisfy this requirement.

4. EXPERIMENTAL RESULTS

The robotic system has been used in *in vitro* experiments using a cadaver mandible, as described previously. It was thus known *a priori* that there were no anatomical changes in initial and subsequent radiographs. Therefore, any changes revealed by registration and subsequent subtraction were due primarily to changes in the imaging geometry.

Three sensorized mouth appliances were constructed to allow the placement of the 3-D sensor and X-ray film at different locations on the jaw. The first mouth appliance was used to image the right first and second premolars and first and second molars. The second mouth appliance allowed the film to be placed behind the central and lateral left and right incisors. The third appliance was used to image the right first, second and third molars.

The next step was to calibrate the GE X-ray system in order to have good contrast in the film. The exposure was fixed at 12/60 of a second, while the current was set at 10 mA and voltage at 70 kVp. Subsequently 57 radiographs were taken using either the 3-D tracker or a mechanical stent for X-ray source-film imaging standardization. In both cases the robotic system carried the X-ray source, and the jaw holding the film and 3-D tracker was moved manually using the motorized platform previously described. After each

Table 2. Comparison of image registration results. (© Shadyside Hospital. Reprinted by permission.)

		3-D tracker-based registration				
Value	Mean	Stnd dev.	X trans (pixel)	Y trans (pixel)	$X(\theta)$	$Y(\theta)$
Avg.	127.25	3.85	2.85	2.59	0.01	0.01
Min.	122.25	3.01	0.10	0.00	0.00	0.00
Max.	132.22	4.67	6.56	10.51	0.05	0.04
		Stent-based registration				
Avg.	127.24	4.27	4.51	3.72	0.02	0.02
Min.	114.14	3.12	0.09	0.01	0.00	0.00
Max.	140.33	6.34	12.70	10.72	0.07	0.06

Table 3. Comparison of subtraction of non-standardized images (straight subtraction) (Levy, 1994). (© Shadyside Hospital, reprinted by permission.)

3-D tracker-based registration		
Value	Mean	Stnd dev.
Avg.	127.24	5.91
Min.	122.25	3.51
Max.	132.41	8.68
Stent-based registration		
Avg.	127.25	7.46
Min.	114.19	3.95
Max.	140.31	13.45

X-ray was taken the robot was homed, and the appliance was removed between classes of X-rays (frontal, or lateral left or right). This was done in order to increase realism by changing the robot path and trajectory for every new film. Additional variables could have been introduced if several jaws and appliances were used (for several 'patients'). However this was beyond of the scope of this stage of our project.

Once the radiographs of the different mandible regions were digitized, they were stored in the database created with the SRUI. A single user performed manual selection of feature points in all X-rays of a given mandible region, as well as image registration and subtraction. This data was stored and analyzed using the SRUI statistical software. The fundamental matrices used in image rectification were then compared to determine which method (stent or robot-based tracking) produced more uniform images. Table 2 shows a summary of the subtraction statistics, the required translation along the X and Y axes, as well as the rotation about these axes, for all radiographs. It is clear that the use of 3-D sensor tracking produced images that needed less compensation than those obtained using stent-based registration.

Another measure of imaging standardization performance was the average and standard deviation in the subtracted image, depending on the registration method. Ideally, the subtracted image should have an average of 127.5 and zero standard deviation, since there were no anatomical changes between images of the same mandible region. As shown in Table 2, both methods produced subtracted images with 127 average intensity, however the variability in both intensity mean and standard deviation was much larger for the images obtained using the mechanical stent. Thus registration results on images using robotic tracking were more uniform than those based on mechanical image standardization.

Figure 4 (Levy *et al.*, 1994) shows two typical examples of subtracted images after standardization. The image to the left was from stent-based image standardization, while the image to the right was based on radiographs of the same mandible area, but using robotic 3-D tracking. It can be seen that the stent-based approach produced false positive bone changes (lighter gray areas), while the robotic system produced better imaging subtraction results.

Further proof of the superiority of the robotic-based imaging standardization are the results from the subtraction of non-standardized images, as detailed in Table 3 (Levy, 1994). These subtraction results summarize the difference between a pair of images, without any subsequent registration by image processing. The standard deviation of the robotic-based subtracted images is much smaller than that of images based on the stent approach. Furthermore, as in the standardized subtraction, the uniformity of results is much better in the robotic case than with the stent approach.

5. CONCLUSIONS AND FUTURE WORK

A proof-of-concept system was developed for robot-based dental subtraction radiography. The system replaces mechanical or 'free hand' attempts to standardize exposure geometry with a non-contact approach using a 3-D position sensor. A Unix-based software environment was created to allow easy menu-driven user interaction with the robotic system, safe operation and easy post-processing of digital images. Results of *in vitro* experimental tests showed the robotic system to be superior to the stent approach in image standardization resulting in smaller differences when both direct and rectified image subtraction are performed. The uniformity of the results using the robotic system was clearly superior to the large variability observed in stent-based image subtraction.

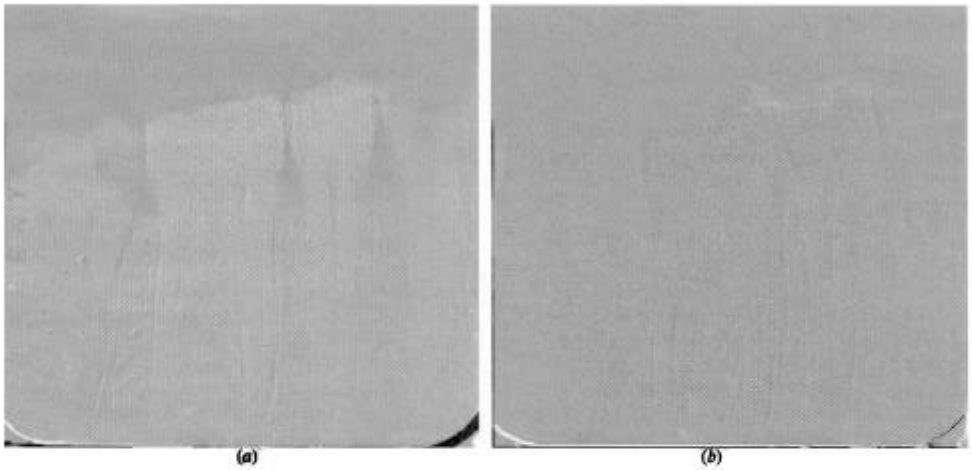

Figure 4. Subtraction images with (**a**) stent and (**b**) robotic image standardization (Levy *et al.*, 1994). (© Shadyside Hospital, reprinted by permission.)

The robotic system used in the present experiments was designed for industrial rather than medical applications. If the present system is reduced to practice in dental offices, then a smaller X-ray source as well as a smaller manipulator could be utilized. This in turn would limit costs and increase patient safety. The improvements in digital radiography may make possible the use of a digital sensor instead of the present analog film. Dental X-ray imaging processing can be automated further by eliminating the film processing and digitization steps used in the present study. The above technological advances, and the steep reduction in computing and robot hardware costs, will make possible the future widespread use of dental robots, and outside high-tech research clinics.

This technology is not expected to replace current routine diagnostic procedures, but it is believed that it can be used for improved diagnostic tests for patient care. One advantage of the robotic system is that the tube motion can be controlled accurately and reproducibly (as shown in this study) to produce plane films of sections of bone in structures of complex topology such as the pelvis or the head and neck (including the jaws). We are currently studying automatic feature point selection to replace the manual procedure used in the experiments described above. This automatic feature point selection will be coupled with robotic control to closely register images taken in rapid succession. Different exposure parameters will be used for detecting changes in bone mineral density due to systemic metabolic bone diseases such as diabetes and osteoporosis. It has been shown recently that the rectification and subtraction procedure can be used with a calibrated step wedge to detect true differences in bone mineral density of 0.1 mg of calcium with either single- or dual-energy radiography (Dunn *et al.*, 1999). This precision is sufficient for diagnosing bone loss in axial and peripheral sites (such as the dentition) which can now be chosen arbitrarily, with the introduction of robotic control of the tube motion.

Programmable tube motion, in conjunction with digital X-ray sensors is furthermore expected to allow the creation of diagnostic procedures using localized computed tomography to reduce patient risk and cost (Dunn *et al.*, 1998). In localized procedures, the robot controls the tube motion so that the minimum number of projections necessary are taken to gather sufficient data to create a complete 3-D reconstruction of the (small) area of interest (van der Stelt *et al.*, 1997).

Since the 3-D pose of plane film radiographs can now be estimated (Ostuni *et al.*, 1996, 1997) both localized computed tomography and tomosynthesis become clinically feasible. Tomosynthesis (van der Stelt *et al.*, 1997) is a procedure to synthesize plane film projections of a 3-D structure from a small set of 'basis' projections taken with the source pose precisely known. Instead of using multiple tube heads to collect the image data, the robot may reposition a single head, insuring uniformity of the incident beams and simultaneously minimizing the cost. Both of these advances, as well as others, are imminent with the introduction of robot control for radiography.

ACKNOWLEDGEMENTS

Research reported here was supported by Grant PHS 1-R03-DE10230 from the National Institute of Health, and by equipment Grants from the University of Medicine and Dentistry of New Jersey and from AT&T Bell Laboratories.

REFERENCES

American Robot Co. (1985a) *Merlin System Operator's Guide*, Version 3.0.

American Robot Co. (1985b) *AR-BASIC*, Version 3.0.

Braegger, U. (1988) Digital imaging in periodontal radiography. *J. Clin. Periodont.*, 15, 551–557.

Braegger, U., Pasquali, L., Weber, H. and Ortman, K. (1989) Computer-assisted densiometric image analysis for assessment of alveolar bone density changes in furcations. *J. Periodont. Res.*, 16, 42–52.

Brown, L. J. and Loe, H. (1993) Prevalence, extent, severity and progression of periodontal disease. *Periodontology 2000*, 2, 57–71.

Burdea, G., Dunn, S. M., Mallik, M. and Immendorf, C. (1991) Real time sensing of tooth position for dental digital subtraction radiography. *IEEE Trans. Biomed. Eng.*, 38, 366–378.

Burdea, G., Dunn, S. M. and Desjardins, D. (1992) Apparatus for taking radiographs used in performing dental subtraction radiography with a sensorized dental mouthpiece, and a robotic system. *US Patent* 5 113 424.

Curry, T. S., Dowdey, J. E. and Murry, R. C. (1984) *Christensen's Introduction to the Physics of Diagnostic Radiology*, 3rd edn, pp. 290–294. Lea & Feibiger, Philadelphia, PA.

Dunn, S. M. (1993) *Digital Standardization of Dental Radiographs*. Vrije Universiteit Press, Amsterdam.

Dunn, S. M., Burdea, G. and Goratowski, R. (1996) Robotic control of intraoral radiography. In Taylor, R. H., Lavallée, S., Burdea, G. and Mösges, R. (eds), *Computer-Integrated Surgery*, pp. 519–528. MIT Press, Cambridge, MA.

Dunn, S. M. and van der Stelt, P. (1998) Feasibility of localized tomography from incomplete data. *J. Dental Res.*, Abstract no 975.

Dunn, S. M., Mol, A., Northington, G. and Giannakopolous, K. (1999) Radiological analysis of tetracycline therapy, *Ann. Periodontol., Proc. Workshop on Non-Antibiotic Properties of Tetracyclines*, at press.

Fisher, E., Ostuni, J., van der Stelt, P. and Dunn, S. M. (1995) The effect of independent film and object rotation on projective geometric standardization of dental radiographs. *Dento Maxillofacial Radiol.*, 24, 5–12.

Genco, R. J. and Loe H. (1993) The role of systemic conditions and disorders in periodontal disease. *Periodontology 2000*, 2, 98–116.

Levy, G. (1994) *Robotic Control for Digital Subtraction Radiography*, MS Thesis, ECE Department, Rutgers University, Piscataway NJ.

Levy, G., Burdea, G., Dunn, S. and Goratowski, R. (1994) Robotic control for dental subtraction radiography. *1st Int. Symp. on Medical Robotics and Computer Assisted Surgery*, Pittsburgh, PA, pp. 334–341.

Ortman, L., Dunford, R., McHenry, K. and Hausmann, E. (1985) Subtraction radiography and computer assisted densitometric analyses of standardized radiographs. *J. Periodont. Res.*, 20, 644–651.

Ostuni, J. and Dunn, S. M. (1996) Motion from three weak perspective images using image rotation. *IEEE Trans. PAMI*, 18, 64–69.

Ostuni, J. and Dunn, S. M. (1997) Measuring registration potential in transmission images. *Comput. Med. Imag. Graphics*, 21, 103–110.

Ostuni, J., Fisher, E., van der Stelt, P. and Dunn, S. M. (1995) Registration of dental radiographs using projective geometry. *Dento Maxillofacial Radiol.*, 22, 199–203.

Quercia, V. and O'Reilly, T. (1993) *X Window System User's Guide*. O'Reilly & Associates Inc., Sebastopol, CA.

Rethman, M., Ruttiman, U., O'Neal, R., Webber, R., Davis, A., Greenstein, G. and Woodyard, S. (1985) Diagnosis of bone lesions by subtraction radiography. *J. Periodont. Res*, 56, 324–329.

Versteeg, K. H., van der Stelt, P. F. and Dunn S. M. (1995) Effect of logarithmic contrast enhancement on subtraction images, *Oral Surg. Oral Med. Oral Pathol. Oral Radiol. Endodontics*, 80, 479–486.

van der Stelt, P. F. and Dunn, S. M. (1997) 3D-Imaging in dental radiology. *IADMFR/CMI '97—Advances in Maxillofacial Imaging*, Louisville, KY, pp. 367–372.